59. Chumakov G D et al., in *Proc. of the Xth IEEE Intern. Pulsed Power Conf., Albuquerque, NM, USA, 1995*
60. Andreev N F et al. *Kvantovaya Elektron.* **34** 381 (2004) [*Quantum Electron.* **34** 381 (2004)]
61. Arbuzov V I et al. *Opt. Zh.* **70** (5) 68 (2003) [*J. Opt. Technol.* **70** 361 (2003)]
62. Voronich I N et al. *Kvantovaya Elektron.* **35** 140 (2005) [*Quantum Electron.* **35** 140 (2005)]
63. Kryukov P G *Kvantovaya Elektron.* **31** 95 (2001) [*Quantum Electron.* **31** 95 (2001)]
64. Piskarskas A, Stabinis A, Yankauskas A *Usp. Fiz. Nauk* **150** 127 (1986) [*Sov. Phys. Usp.* **29** 869 (1986)]
65. Andreev N F et al. *Pis'ma Zh. Eksp. Teor. Fiz.* **79** 178 (2004) [*JETP Lett.* **79** 144 (2004)]

PACS numbers: 07.55.Db, **64.30.–t**, **74.25.–q**
DOI: 10.3367/UFNe.0181.201104n.0441

Research in ultrahigh magnetic field physics

G V Boriskov, A I Bykov, M I Dolotenko, N I Egorov, Yu B Kudasov, V V Platonov, V D Selemir, O M Tatsenko

1. Introduction

The history of the achievements of the All-Russian Research Institute of Experimental Physics (VNIIEF in *Russ. abbr.*) in the field of ultrahigh magnetic field (UHMF) generation and applications in fundamental physical studies begins in 1952, when Andrey D Sakharov put forward the idea of magnetic cumulation as one of the possible methods for achieving a controlled thermonuclear reaction [1]. He also proposed two types of magnetocumulative generators of UHMFs (MC-1) and energy (MC-2) [1, 2]. In the first of them, a special device produces the initial axial magnetic field flux in the cavity of a cylindrical metal shell (liner). A converging detonation wave is initiated in a circular explosive charge surrounding the liner so that it arrives at the external boundary of the liner at the instant of time when the initial magnetic field in the liner achieves a maximum. Under the action of pressure of the detonation products, the liner collapses to the center, compressing the initial magnetic flux. If the compression is rapid enough, the magnetic flux in the cavity is preserved, and the magnetic field strength on the liner axis increases inversely proportionally to the squared radius of the liner, achieving a few megagausses. The chemical energy of the explosive is transformed into the magnetic field energy through the kinetic energy of the liner.

Extensive attempts made in many countries to reproduce UHMFs by the explosive compression of a magnetic flux revealed unexplainable difficulties in obtaining magnetic fields exceeding 3 MG, which resulted in the termination of work in this field.

G V Boriskov, A I Bykov, M I Dolotenko, N I Egorov, Yu B Kudasov, V V Platonov, V D Selemir, O M Tatsenko Federal State Unitary Enterprise 'Russian Federal Nuclear Center — All-Russian Research Institute of Experimental Physics', Sarov, Nizhny Novgorod region, Russian Federation. E-mail: selemir@vniief.ru

Uspekhi Fizicheskikh Nauk **181** (4) 441–447 (2011)
DOI: 10.3367/UFNr.0181.201104n.0441
Translated by M Sapozhnikov; edited by A Radzig

2. MC-1 cascade generator

A group of researchers at VNIIEF headed by A I Pavlovskii proposed and realized a number of concepts supplementing and developing the magnetic cumulation idea and solved the problem of the reproducible generation of UHMFs.

First, it was proposed to make the shells of the MC-1 generator from a material with a controllable electrical conduction. Such a material in the initial state is either completely nonconducting or conducts current only in one direction. At the required instant, a shock wave is passed through the material, making it conducting in all directions. For example, such a material can be produced from closely packed parallel isolated copper wires glued with an epoxy compound.

Second, unique solenoids of the initial magnetic field in the MC-1 generator were constructed in the form of a cylinder made of a composite material with the internal layer containing wires forming a multiple (≈ 500 entry wires), multilayer (7–13 winding layers) solenoid (Fig. 1). This made it possible to reliably obtain high magnetic fluxes and use the solenoid as a liner: after the passage of a shock wave from an explosive charge, the wires are connected up to form a continuous conducting cylinder capturing and compressing the magnetic flux [3].

Third, because the high initial magnetic flux in the wire solenoid provided UHMF generation in large volumes, the X-ray diffraction analysis of the longitudinal cross section of the MC-1 generator showed that the magnetic field strength is mainly restricted by the instability of the matter–field interface during the deceleration of the shell by the pressure of the strengthened magnetic field [4].

Fourth, the cascade principle of magnetic field strengthening was proposed, which removed this restriction, stopped the development of instabilities, and provided the reproducible generation of multimegagauss magnetic fields [5, 6]. One or two cylindrical cascade shells made of the same composite are located coaxially to the shell solenoid. In the initial state, the cascade shells easily transmit the amplified magnetic field flux inside, but each time the internal boundary of the liner can lose its stability, the liner is replaced by a new one, which compresses the magnetic flux when conduction appears in the cascade material after the impact of one cascades with the other.

The MC-1 cascade ten-megagauss magnetic field generator was developed for many years of research work and then produced in batches (see Fig. 1) [7, 8]. The basic

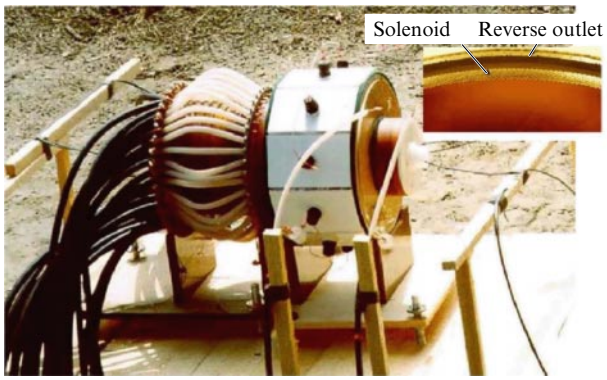

Figure 1. Appearance of the MC-1 cascade generator prepared for an explosion experiment. The inset shows a part of the cross section of the solenoid shell of the MC-1 generator.

parameters of the generator are as follows: the initial internal diameter of the shell is 139 mm, the explosive mass is 16 kg, and the initial magnetic field is up to 250 kG. The second and third cascades of the generator with the internal and external diameters of 28 and 35 mm and 12 and 17 mm, respectively, can be made of a wire composite or a composite based on a finely divided metal powder and a polymer binder [9].

This generator makes up a rather simple and comparatively inexpensive device intended for explosion experiments, which was adjusted to a device made in large numbers (by now a few hundred such generators has been manufactured) with limiting, record parameters. Relatively large UHMF volumes make it possible to study simultaneously several samples even at cryogenic temperatures, while the cylindrical geometry and 'transparency' of the magnetic field allow studying matter under extreme conditions applying various methods, including optical. This generator was used in various investigations, in particular, in the international experiments Dirac in the USA, and Kapitza at the Scientific and Technical Center of High Energy Density Physics of Directed Radiation Fluxes at VNIIEF [10, 11].

In the 'large' MC-1 generator, with approximately doubled explosive charge dimensions (the explosive mass was increased approximately eightfold) and built at VNIIEF, a single-cascade gasdynamic liner-acceleration system with a steel striker is utilized and magnetic field strengths of about 20 MG were detected in several experiments, while in one experiment a record-high magnetic field strength of about 28 MG was achieved (the field energy density was ≈ 3 MJ cm^{-3}!) [12]. Experiments with large generators showed that these experiments are much more complicated and expensive and their cost should be justified by the scientific importance of the studies performed using them.

3. Solid state physics in ultrahigh magnetic fields

Ultrahigh magnetic fields can be efficiently used for solid-state physics studies. Some results obtained by the authors with the help of UHMFs produced by the MC-1 generator were presented in reviews [13, 14].

Ultrahigh magnetic fields attracted considerable interest at once after the discovery of high-temperature superconductivity because high critical temperatures should correspond to high critical magnetic fields B_c, which are the fundamental characteristic of the superconducting state. Of interest are also phase transitions between different states of the superconducting phase itself (for example, the 'vortex glass–vortex lattice' transition). Our first experiments showed that the critical field in $YBa_2Cu_3O_{7-x}$ at 4.2 K exceeds 200 T [15]. The later-developed contactless high-frequency methods for measuring the admittance were applied for precision measurements of the conduction of $YBa_2Cu_3O_{7-x}$ films in UHMFs when the crystallographic c-axis was oriented perpendicular to the magnetic field vector. These measurements were performed in a joint Russian–American series of experiments at VNIIEF and Los Alamos National Laboratory [16]. One can see from Fig. 2 that the imaginary part of the film conduction dominated at low temperatures in weak fields, i.e., vortices were located at the pinning centers. In the field ≈ 75 T (point A), the real part of the conduction began to rapidly increase, while its imaginary part began to decrease. This is caused by lattice melting. In fields above 210 T, only a small part of the pinning vortices remains (the conduction has the imaginary part), and the sample is found

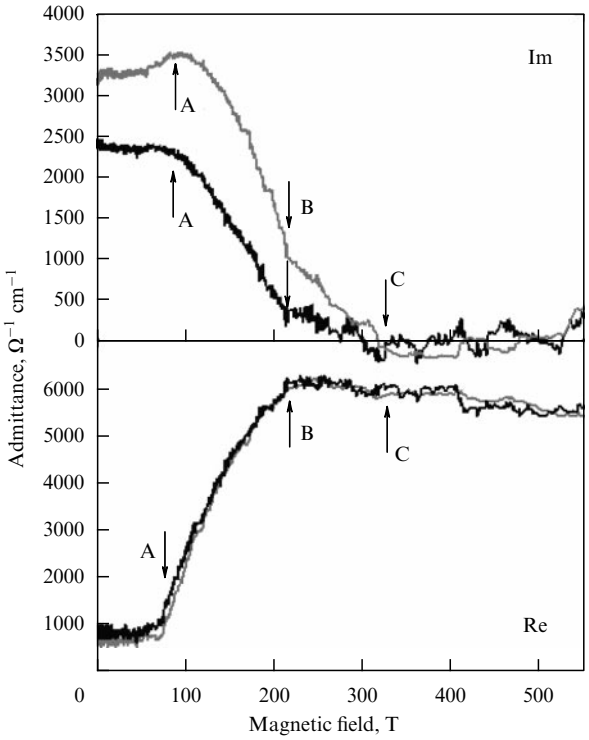

Figure 2. Admittance of $YBa_2Cu_3O_{7-x}$ at a frequency of 94 GHz (the grey and dark curves are measured by the signal transmission and refection methods, respectively).

predominantly in the viscous flow motion regime. The disappearance of the imaginary part of the conduction and flattening out of its real part (point C) correspond to the second critical field $B_{c2}(8 \pm 3\ \mathrm{K}) = 340 \pm 40$ T.

The study of semiconductors in UHMFs makes it possible to determine the energy band diagram in the range from a few dozen to a few hundred meV. Semiconductor samples with low carrier mobility or a high concentration of defects or impurities can also be investigated. As a rule, it has been possible to determine in such experiments the effective electron mass in the conduction band, the Luttinger parameters in the valence band, and g factors for electrons and holes. All these quantities are functions of the electron energy, which can be determined only in UHMFs. (In weak magnetic fields, it is possible to measure the values of these functions corresponding to the band edges because the electron cyclotron energy is much smaller than the band width.)

The cyclotron resonance in a cubic high-energy-gap GaN semiconductor was measured in joint experiments with a group led by M von Ortenberg of Humboldt University of Berlin. This semiconductor is promising for applications in radiation sources. However, its electronic properties in this phase are poorly studied because of the absence of high-purity samples and low carrier mobility. Three resonance peaks were revealed in magnetic fields of 90, 270, and 410 T, which gave the effective masses and dispersion of electronic states [17].

In quantum-well InGaAs/GaAs heterostructures, the fundamental cyclotron resonance of holes and interband magnetoabsorption were studied. These heterostructures were grown at the Institute of Microstructure Physics, Russian Academy of Sciences (Nizhny Novgorod). When transmission is measured at a wavelength of 0.87 μm, which exactly corresponds to the GaAs band gap (quantum energy of 1.425 eV), the sample becomes transparent only in the field

of 50 T. For the same reason, the sample becomes transparent at 0.83 μm in the field of 150 T, although the calculation taking exciton effects into account gives 100 T [18]. In stronger magnetic fields, absorption bands in the range from 230 to 350 T were observed. They are caused by transitions from the two upper (spin-split) Landau levels in the first hole subband to the two lower Landau levels in the first electron subband, and by similar transitions between second subbands (shifted by approximately 50 T to the region of the lower magnetic fields), taking exciton effects into account. The same transitions between the first subbands at $\lambda = 0.87$ μm are responsible for the transmission minimum at 150 T and a singularity observed at 210 T. The cyclotron absorption line observed in these experiments in the magnetic field $B \approx 80$ T can be related to the *intersubband* cyclotron resonance, namely, to the transition from the $3a_1$ upper Landau level of holes in the quantum well in the first hole subband to the $4a_3$ level belonging to the third subband.

Among the family of low-energy-gap semiconductors, iron monosilicide (FeSi) is distinguished by its unusual properties. For example, the sum rule violation in FeSi is broadly discussed in optical spectroscopy: metallization with increasing temperature occurs much earlier than would be expected from band calculations, etc. Because the Zeeman splitting in UHMFs is comparable to the band gap in the spectrum of the s, p, and d electrons in FeSi, equal to 0.11 eV, those fields exceeding 100 T can drastically restructure the electronic spectrum and, therefore, can be used as a powerful tool for studying the electronic structure of low-energy-gap semiconductors.

The induction method with the use of compensation coils proved to be very convenient for studying the magnetization in experiments with the MC-1 [19]. The induced signal is proportional to the differential magnetization multiplied by the magnetic field growth rate, which achieves a record-high value in the MC-1 generator ($\approx 10^6$ T s^{-1}), thus providing the high sensitivity of sensors in the entire measurement range. In pulsed magnetic fields, diamagnetic currents are induced along with magnetization, which allows the conduction to be measured as well. For this purpose, samples of two types are used: in the form of a pure FeSi powder (a single crystal was ground in a porcelain mortar to obtain granules ≈ 100 μm in size), and in the form of a mixture of a single-crystal powder with polymerized polymethyl methacrylate (single-crystal FeSi granules in a dielectric matrix).

A sharp peak (Fig. 3) observed in both samples in the magnetic field of 355 ± 20 T at 4.2 K points to the transition to the conducting phase [19]. The calculated jump in the magnetic moment is $(0.95 \pm 0.2)\,\mu_B$ per Fe atom, which suggests that saturation is achieved due to a single transition rather than due to the two successive phase transitions predicted in some theoretical papers.

The main subjects of studies in magnetics were spin reorientation processes in ultrahigh magnetic fields. Spin-flip and spin-flop transitions in MnF_2, $KMnF_3$, and $FeBO_3$ antiferromagnetics and the step magnetization curve of a multisublattice $Ho_{0.7}Y_{2.3}Fe_5O_{12}$ magnet were studied in Ref. [20]. A magnetic field can distort the electronic structure of the ground state, resulting in induced band magnetism.

The level crossover in the paramagnetic $YbPO_4$, $TmPO_4$, $ErVO_4$, and $PrVO_4$ zircons was studied by the induction method at 4.2 K in magnetic fields of up to 400 T [21, 22]. Figure 4 depicts the experimental and theoretical dependences of the magnetic susceptibility dM/dH for $YbPO_4$ for

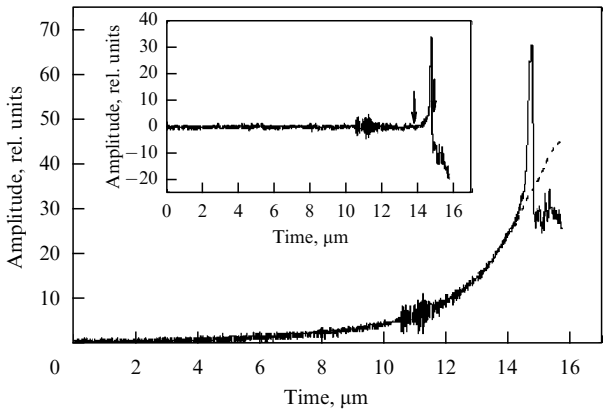

Figure 3. Output signal of an inductive sensor with an FeSi powder at the initial temperature of 4.2 K (solid curve) and the scaled signal of an inductive field sensor (dashed curve). The inset displays a signal purified from the background $\propto \partial B/\partial t$; the arrows show the integration interval for determining the magnetic moment jump.

a magnetic field directed along the tetragonal [001] axis. The broad susceptibility maxima at $B_c \approx 280$ and 50 T are related to the crossover of the energy levels of Yb^{3+} and Pr^{3+} ions. Calculations of the isothermal and adiabatic magnetization of $YbPO_4$ made it possible to determine a change in the sample temperature during experiments. The sample is first heated by approximately 25 K and then is cooled by approximately 20 K in the region of the crossover fields. The sign of the 'elementary' magnetocaloric effect is determined by the sign of the derivative $\partial M/\partial T|_{H=\text{const}}$.

Ultrahigh magnetic fields can induce a change in the valence in some compounds containing Ce, Sm, Eu, Tm, and Yb rare-earth ions. Such a behavior of these compounds is caused by the location of the 4f level near the Fermi level. In particular, the mixed-valence state appears in $EuNi_2Si_2$ and $EuNi_2Ge_2$ solutions. The $4f^6$ Eu^{3+} ion in $EuNi_2Si_2$ is nonmagnetic, whereas the magnetic moment of the $4f^7$ Eu^{2+} ion in $EuNi_2Ge_2$ amounts to $7\,\mu_B$. In $EuNi_2(Si_{1-x}Ge_x)_2$ compounds, the valence transition is induced from the mostly trivalent-ion state to the mostly bivalent-ion state, which is accompanied by a jump in the magnetic moment. The fields of magnetoinduced valence transitions were experimentally determined for these compounds in the range of Ge concentrations up to $x = 0.5$. The critical filed B_c linearly grows with decreasing concentration in the entire concentration range [23].

The study of the Faraday effect in $Tb_3Ga_5O_{12}$ terbium gallate garnet (the energy spectrum of its magnetic subsystem has been thoroughly investigated in static fields) in UHMFs, which increase in the MC-1 generator at a rate of 10^7–10^8 T s^{-1}, was performed to determine the value of the magnetocaloric effect, which is important from the methodical point of view. It was shown that the sample temperature during the adiabatic magnetization in a field of 75 T reached 35 K and no unexpected increase in the temperature occurred in pulsed magnetic fields [23].

4. Isentropic compression of matter by the ultrahigh magnetic field pressure

The investigation of the behavior of materials, first and foremost their equations of state, at ultrahigh pressures is one of the interesting problems of high energy density physics [24, 25]. Of special interest here is the low-temperature region,

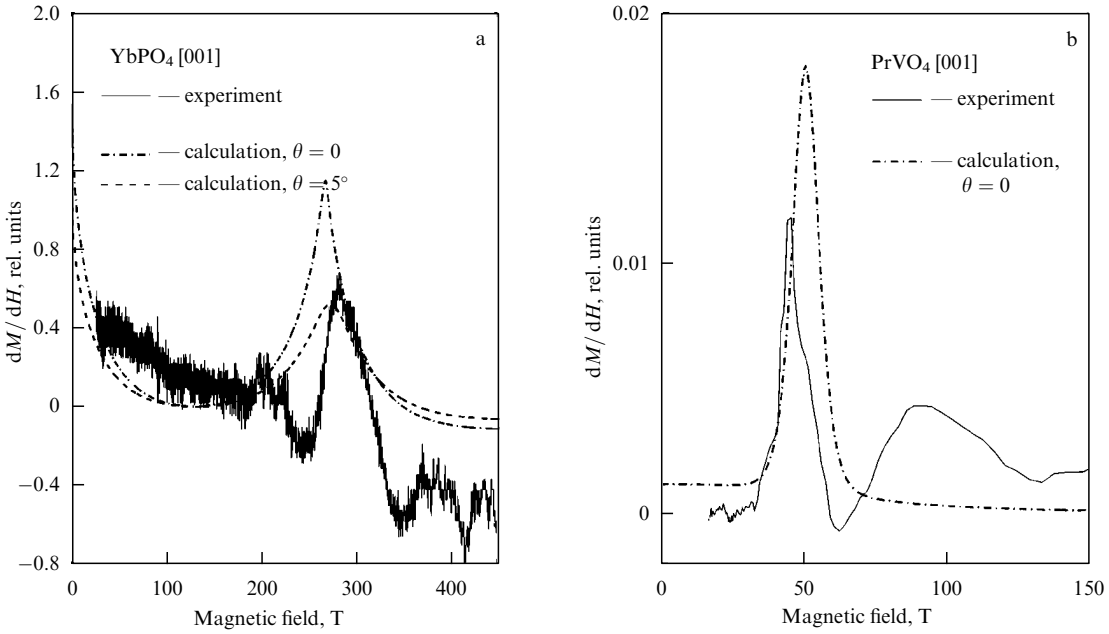

Figure 4. Dependences of the differential susceptibility dM/dH for $YbPO_4$ (a) and $PrVO_4$ (b) for a magnetic field oriented near the tetragonal [001] axis (θ is the reorientation angle).

which is important not only, for example, for understanding the structure and evolution of giant planets, but also for verifying fundamental theoretical concepts.

High and ultrahigh pressures are produced by two basic methods, static and dynamic, which supplement each other. In statics, the regime of isothermal compression is realized, as a rule, at comparatively low temperatures ($T < 1000$ K) [26]; the equations of state are studied at static pressures below 1.5 Mbar to avoid the destruction of samples. (In addition, the growth of pressure is limited by the strength of the anvil material.) On the other hand, the temperature can reach a few dozen thousand degrees in the dynamic shock-wave regime, but in this case the 'cold' pressure does not exceed even 0.5 Mbar (see, for example, Ref. [27]). Another dynamic method is the isentropic compression of matter in a chamber whose external surface is subjected to the action of a uniform, gradually increasing external pressure [28]. The thermal component of the total pressure, unlike that in the shock-wave method, will be considerably smaller as in the static method, than the cold component, and at a low initial temperature of a material under study its isentrope will be close to the zero isotherm. At present, the characteristics of substances in the region of *low temperatures and ultrahigh* (*multimegabar*) *pressures* can be efficiently determined only by the isentropic compression method. The properties of materials in this region are studied at VNIIEF by the method of *isentropic compression by ultrahigh magnetic field pressure* [29, 30]. The experimental results obtained by this method are mainly related to the construction of zero isotherms of the hydrogen isotopes — protium and deuterium. (Notice, by the way, that researchers at VNIIEF were among the first to study hydrogen at ultrahigh pressures [31–33].)

Interest in studying the thermodynamic and kinetic properties of hydrogen is not accidental and is caused by the wide abundance of hydrogen in the Universe and its practical importance as one of the basic elements for future energy production. In addition, a number of unusual, exotic properties of hydrogen have been predicted: the high-temperature superconductivity of its metal phase [34], the temperature maximum in the melting curve [35–37], and the existence of a two-component superfluid and superconducting liquid [38].

The method that we apply is based on a compression device containing an MC-1 magnetocumulative generator [7], a cylindrical compression chamber [39], and a cryogenic device [40] (Fig. 5). The compression chamber is formed by a thick-walled copper compressing tube and massive end caps. The standard sample and sample under study are located coaxially under the compressing tube (at the center). The cryogenic device, containing a liquid helium vessel and an evacuated cryoduct, is destined for preliminary cooling the gas under study to the solid state ($T_0 \approx 5$ K). Under the action of the excess pressure produced in the helium vessel, helium rises upward through the cryoduct and gradually cools the compression chamber together with its content. During the discharge of a high-power capacitor bank to the generator solenoid in its cavity, in the gap between the solenoid and compressing tube, an initial magnetic flux is produced. The magnetic field in the gap is increased up to a few megagausses during the operation of the MC-1 generator and exerts a uniform magnetic pressure $B^2/8\pi$ on the external surface of the compression chamber. As a result, the chamber tube collapses without the generation of shock waves and compresses (for ≈ 15 μs) the materials inside it up to a few megabars.

An important and substantial part of the studies is the numerical simulation of processes proceeding in the compression device with the help of applied program packages developed at VNIIEF [41–43]. One of the main goals of simulations is to determine the compression chamber geometry and initial dimensions and the initial field of the MC-1 generator that would provide minimal pressure gradients in the working region of the compression chamber. The results of calculations were also used in the development of the X-ray diffraction method for measuring the dimensions [44]. Finally, the calculated results are also

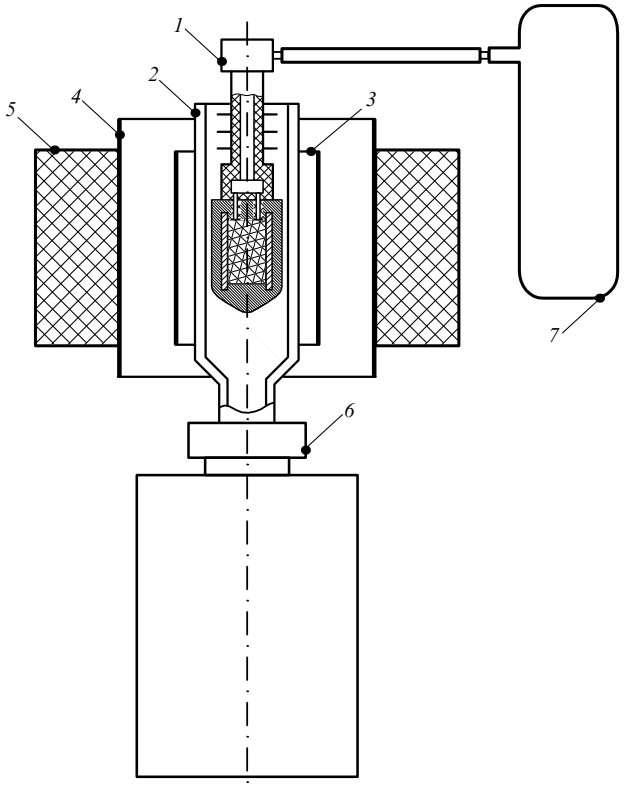

Figure 5. Schematic of the compression device: (*1*) cryogenic vessel with a compression chamber filled with the material under study; (*2*) cryoduct; (*3*) second cascade of the MC-1 generator; (*4*) solenoid of the initial field of the generator (first cascade); (*5*) circular explosive charge; (*6*) liquid helium vessel, and (*7*) container with the gas under study.

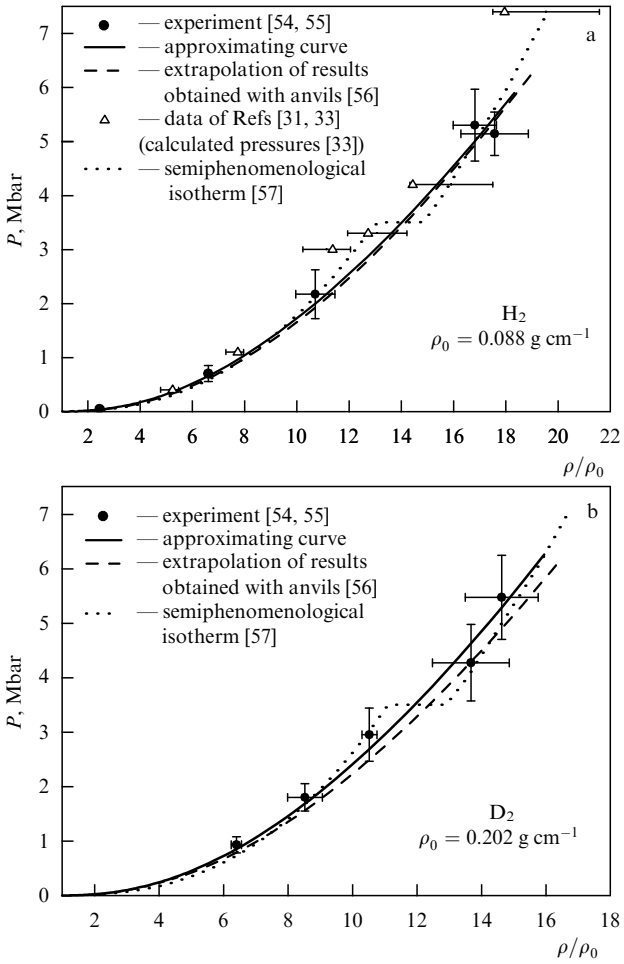

Figure 6. Pressure–compression diagrams for protium (a) and deuterium (b).

employed to analyze experimental data and estimate the gradient correction in measurements of pressure in the sample under study.

The density ρ and pressure P of a compressed material are determined in the following way. The central part of an experimental device is illuminated by a bremsstrahlung pulse from a BIM-234 betatron [45, 46] and the image is recorded on an X-ray film. The X-ray pattern is recorded when pressure in the compression chamber reaches ultrahigh values. The sizes and, hence, compressibilities of the sample under study and standard sample are determined from the processed images in X-ray patterns. The sample density during X-ray pattern recording can be easily obtained from the known compressibility and initial density ρ_0 of the sample. Pressure in the measurement standard can be determined from its density with the aid of its known isentrope. Then, taking into account small calculation corrections, pressure in the sample under study can also be determined. The best material for the standard is aluminium, for which the most comprehensive statistical data covering the required pressure range have been gathered and processed [47–53]. To determine accurately enough the dimensions of compressed samples from an X-ray pattern, a thin layer of a highly dense material should be placed on the boundaries between the samples and between samples and the compressing tube. We utilized an alloy containing 95% tungsten. Thus, we find from the X-ray pattern a point at the $P-\rho$ plane for the material under study. By changing the X-ray recording time from experiment to experiment, we obtain a set of points corresponding to the 'cold' isentrope of the material.

By utilizing the compression devices and measurement methods described above, researchers at VNIIEF performed experiments [54, 55] to obtain the zero isotherms for protium and deuterium in the pressure range from 1 to 5 Mbar. The experimental data obtained for H_2 and D_2 are presented in the $P-\rho/\rho_0$ plane in Fig. 6. The solid curve shows the approximation of experimental data. The zero isotherm obtained in experiments with diamond anvils [56] and extrapolated to the megabar region is illustrated by the dashed curve. The dotted curve was proposed in Ref. [57] for the molecular and atomic phases of protium and deuterium. The data obtained in Refs [54, 55] reveal no dramatic deviations in the behavior of the zero isotherms. Some scatter of points in the diagram at pressures exceeding 4 Mbar may be caused by a polymorphic transformation in the lattice or even by the lattice melting produced by pressure [35]. One can see that the points [54, 55] agree within the measurement error with the zero isotherm [56], although they lie somewhat higher at pressures above 1 Mbar. They are also consistent with the semiphenomenological isotherm [57] based on experiments [31–33] on the quasi-isentropic compression of initially gaseous protium[1] (Fig. 6a). However,

[1] The states of the matter obtained in Refs [31–33] correspond to the calculated temperatures exceeding 2000 K [33]. Recent experiments with diamond anvils [36, 37] demonstrate a turn in the melting curve of protium near $T = 1000$ K, and therefore results [31–33] are related to the dense heated matter rather than to the 'cold' matter.

according to Ref. [57], in the pressure region from 3 to 4 Mbar the crystal should undergo a transition from the molecular to the atomic phase with a considerable density jump ($\approx 14\%$). (According to Ref. [56], the transition pressure exceeds 6 Mbar and the density jump will be a few times smaller.) To determine reliably the run of the zero isotherm in this pressure range, it is necessary to perform additional experiments with the improved accuracy of measuring the sample size. Notice also that the compression curve of the static lattice of protium and deuterium constructed in Ref. [55] based on experimental results is consistent with *ab initio* calculations [58–62].

Finally, it should be emphasized that the investigation method described above can also be used to construct the 'cold' compression curves for many other materials consisting of elements with small atomic numbers, such as helium, lithium, graphite, water, and hydrides of light metals.

5. Conclusion

The idea of the magnetic cumulation of energy proposed by Andrey D Sakharov was developed for many years at VNIIEF to the level of a physical method for obtaining ultrahigh magnetic fields, based on the deep understanding of underlying physical processes. The designs of cascade generators of ultrahigh magnetic fields in the 10- and 20-MG ranges have been worked out. The developed method has been introduced into scientific studies and has been used for systematic fundamental investigations in the fields of solid state physics (optical, magnetic, and transport properties of matter) and the physics of extreme states of matter (isentropic compression by megabar pressures). The results of these studies have been reported at International Megagauss Conferences, two of which, the seventh and ninth, were organized by researchers at VNIIEF [63, 64].

References

1. Sakharov A D et al. *Dokl. Akad. Nauk SSSR* **165** 65 (1965) [*Sov. Phys. Dokl.* **10** 1045 (1966)]
2. Sakharov A D *Usp. Fiz. Nauk* **88** 725 (1966) [*Sov. Phys. Usp.* **9** 294 (1966)]
3. Pavlovskii A I et al. *Prib. Tekh. Eksp.* (5) 195 (1979)
4. Pavlovskii A I et al. *Pis'ma Zh. Tekh. Fiz.* **9** 1360 (1983)
5. Pavlovskii A I et al. *Pis'ma Zh. Eksp. Teor. Fiz.* **38** 437 (1983) [*JETP Lett.* **38** 529 (1983)]
6. Pavlovskii A I et al., in *Sverkhsil'nye Magnitnye Polya. Fizika. Tekhnika. Primenenie* (Ultrahigh Magnetic Fields. Physics. Technique. Application) (Eds V M Titov, G A Shvetsov) (Moscow: Nauka, 1984) p. 14
7. Pavlovskii A I et al., in *Sverkhsil'nye Magnitnye Polya. Fizika. Tekhnika. Primenenie* (Ultrahigh Magnetic Fields. Physics. Technique. Application) (Eds V M Titov, G A Shvetsov) (Moscow: Nauka, 1984) p. 19
8. Bykov A I et al. *Physica B* **216** 215 (1996)
9. Dolotenko M I et al., RF Patent No. 2065247; *Byull. Izobret.* (8) 107 (1996)
10. Tatsenko O M, Selemir V D, in *Megagauss Magnetic Field Generation, its Application to Science and Ultra-High Pulsed-Power Technology*: *Proc. of the VIIIth Intern. Conf. on Megagauss Magnetic Field Generation and Related Topics* (Ed. H J Schneider-Muntau) (Hackensack, NJ: World Scientific, 2004) p. 207
11. Selemir V D, Tatsenko O M, Platonov V V, in *Proc. of the X Intern. Conf. on Megagauss Magnetic Field Generation and Related Topics* (Ed. M von Ortenberg) (Berlin, 2004) p. 219
12. Boyko B A et al., in *12th IEEE Intern. Pulsed Power Conf., Monterey, Calif., USA, 1999, Digest of Technical Papers* (Eds C Stallings, H Kirbie) (New York: IEEE, 1999) p. 746
13. Zvezdin A K et al. *Usp. Fiz. Nauk* **168** 1141 (1998) [*Phys. Usp.* **41** 1037 (1998)]
14. Zvezdin A K et al. *Usp. Fiz. Nauk* **172** 1303 (2002) [*Phys. Usp.* **45** 1183 (2002)]
15. Pavlovskii A I et al. *Physica C* **162 – 164** 1659 (1989)
16. Bykov A I et al. *Sverkhprovodimost Fiz. Khim. Tekh.* **8** (1) 37 (1995)
17. Puhlmann N et al. *Physica B* **294 – 295** 447 (2001)
18. Gavrilenko V I, in *Proc. of the 14th Intern. Symp. "Nanostructures: Physics and Technology", St. Petersburg, Russia, 2006*, p. 166
19. Kudasov Yu B et al. *Pis'ma Zh. Eksp. Teor. Fiz.* **68** 326 (1998) [*JETP Lett.* **68** 350 (1998)]
20. Zvezdin A K et al., in *Itinerant Electron Magnetism*: *Fluctuation Effects* (Eds D Wagner, W Brauneck, A Solontsov) (Dordrecht: Kluwer Acad. Publ., 1998) p. 285
21. Kirste A et al. *Physica B* **336** 335 (2003)
22. Kazei Z A et al. *Physica B* **346 – 347** 241 (2004)
23. Levitin R Z et al. *Fiz. Tverd. Tela* **44** 2013 (2002) [*Phys. Solid State* **44** 2107 (2002)]
24. Zel'dovich Ya B, Raizer Yu P *Fizika Udarnykh Voln i Vysokotemperaturnykh Gidrodinamicheskikh Yavlenii* (Physics of Shock Waves and High-Temperature Hydrodynamic Phenomena) (Moscow: Nauka, 1966) [Translated into English (Mineola, NY: Dover Publ., 2002)]
25. Fortov V E *Ekstremal'nye Sostoyaniya Veshchestva* (Extreme States of Matter) (Moscow: Fizmatlit, 2009); *Extreme States of Matter on Earth and in the Universe* (Berlin: Springer, 2011)
26. Jayaraman A *Rev. Mod. Phys.* **55** 65 (1983)
27. Trunin R F et al. *Zh. Tekh. Fiz.* **76** (7) 90 (2006) [*Tech. Phys.* **51** 907 (2006)]
28. Godwal B K, Sikka S K, Chidambaram R *Phys. Rep.* **102** 121 (1983)
29. Pavlovskii A I et al., in *Megagauss Physics and Technology* (Ed. P J Turchi) (New York: Plenum Press, 1980) p. 627
30. Pavlovskii A I et al., in *Megagauss Technology and Pulsed Power Applications. Proc. of the Fourth Intern. Conf. on Megagauss Magnetic Field Generation and Related Topics* (Eds C M Fowler, R S Caird, D J Erickson) (New York: Plenum Press, 1987) p. 255
31. Grigor'ev F V et al. *Pis'ma Zh. Eksp. Teor. Fiz.* **16** 286 (1972) [*JETP Lett.* **16** 201 (1972)]
32. Grigor'ev F V et al. *Zh. Eksp. Teor. Fiz.* **69** 743 (1975) [*Sov. Phys. JETP* **42** 378 (1975)]
33. Grigor'ev F V et al. *Zh. Eksp. Teor. Fiz.* **75** 1683 (1978) [*Sov. Phys. JETP* **48** 847 (1978)]
34. Ashcroft N W *Phys. Rev. Lett.* **21** 1748 (1968)
35. Bonev S A et al. *Nature* **431** 669 (2004)
36. Deemyad S, Silvera I F *Phys. Rev. Lett.* **100** 155701 (2008)
37. Eremets M I, Troyan I A *Pis'ma Zh. Eksp. Teor. Fiz.* **89** 198 (2009) [*JETP Lett.* **89** 174 (2009)]
38. Babaev E, Sudbø A, Ashcroft N W *Phys. Rev. Lett.* **95** 105301 (2005)
39. Boriskov G V et al., in *"Megagauss-XI", Proc. of the Eleventh Intern. Conf. on Megagauss Magnetic Field Generation and Related Topics* (Eds Ivor Smith, Bucur Novac) (London, 2007) p. 269
40. Boriskov G V et al., in *Proc. of 2006 Intern. Conf. on Megagauss Magnetic Field Generation and Related Topics* (Eds G F Kiuttu, R E Reinovsky, P J Turchi) (Piscataway, NJ: IEEE, 2007) p. 465
41. Boriskov G V, Timareva V I, in *VIII Kharitonovskie Chteniya po Problemam Fiziki Vysokikh Plotnostei Energii* (VIII Khariton Readings on Problems of High Energy Density Physics) (Sarov: FGUP "RFYaTs – VNIIEF", 2006) p. 516
42. Boriskov G V, Timareva V I, in *VIII Kharitonovskie Chteniya po Problemam Fiziki Vysokikh Plotnostei Energii* (VIII Khariton Readings on Problems of High Energy Density Physics) (Sarov: FGUP "RFYaTs – VNIIEF", 2006) p. 509
43. Boriskov G V, Timareva V I, Sokolov S S, in *X Kharitonovskie Chteniya po Problemam Fiziki Vysokikh Plotnostei Energii, Sarov, 11 – 14 Marta, 2008* (X Khariton Readings on Problems of High Energy Density Physics, 11 – 14 March, 2008) (Sarov: FGUP "RFYaTs–VNIIEF", 2008) p. 285

44. Pavlov V N et al., in *XII Intern. Conf. on Megagauss Magnetic Field Generation and Related Topics. Abstracts* (Ed. G A Shvetsov) (Novosibirsk: Lavrentyev Institute of Hydrodynamics, 2008) p. 123
45. Pavlovskii A I et al. *Dokl. Akad. Nauk SSSR* **160** 68 (1965) [*Sov. Phys. Dokl.* **10** 30 (1965)]
46. Kuropatkin Yu P et al., in *11th IEEE Pulsed Power Conf. Digest of Technical Papers* (Eds G Cooperstein, I Vitkovitsky) (Piscataway, NJ: IEEE, 1997) p. 1663
47. Al'tshuler L V et al. *Zh. Eksp. Teor. Fiz.* **38** 790 (1960) [*Sov. Phys. JETP* **11** 573 (1960)]
48. Simonenko V A et al. *Zh. Eksp. Teor. Fiz.* **88** 1452 (1985) [*Sov. Phys. JETP* **61** 869 (1985)]
49. Al'tshuler L V, Brusnikin S E, Kuz'menkov E A *Prikl. Mekh. Tekh. Fiz.* (1) 134 (1987) [*J. Appl. Mech. Tech. Phys.* **28** 129 (1987)]
50. Nellis W J et al. *Phys. Rev. Lett.* **60** 1414 (1988)
51. Greene R G, Luo H, Ruoff A L *Phys. Rev. Lett.* **73** 2075 (1994)
52. Kalitkin N N, Kuz'mina L V, in *Udarnye Volny i Ekstremal'nye Sostoyaniya Veshchestva* (Shock Waves and Extreme States of Matter) (Eds V E Fortov, L V Al'tshuler, R F Trunin, A I Funtikov) (Moscow: Nauka, 2000) p. 107
53. Trunin R F et al., in *Eksperimental'nye Dannye po Udarno-Volnovomu Szhatiyu i Adiabaticheskomu Rasshireniyu Kondensirovannykh Veshchestv* (Experimental Data on Shock Wave Compression and Adiabatic Expansion of Condensed Matter) (Ed. R F Trunin) (Sarov: RFYaTs – VNIIEF, 2006) p. 24
54. Boriskov G V et al. *J. Phys. Conf. Ser.* **121** 072001 (2008)
55. Boriskov G V et al. *Contrib. Plasma Phys.,* DOI 10.1002/ctpp.201010106 (2010)
56. Loubeyre P et al. *Nature* **383** 702 (1996)
57. Kopyshev V P, Urlin V D, in *Udarnye Volny i Ekstremal'nye Sostoyaniya Veshchestva* (Shock Waves and Extreme States of Matter) (Eds V E Fortov, L V Al'tshuler, R F Trunin, A I Funtikov) (Moscow: Nauka, 2000) p. 297
58. Barbee T W (III), Cohen M L, Martins J L *Phys. Rev. Lett.* **62** 1150 (1989)
59. Kaxiras E, Guo Z *Phys. Rev. B* **49** 11822 (1994)
60. Natoli V, Martin R M, Ceperley D M *Phys. Rev. Lett.* **70** 1952 (1993)
61. Natoli V, Martin R M, Ceperley D *Phys. Rev. Lett.* **74** 1601 (1995)
62. Pierleoni C, Ceperley D M, Holzmann M *Phys. Rev. Lett.* **93** 146402 (2004)
63. Chernyshev V K, Selemir V D, Plyashkevich L N (Eds) *Megagauss and Megaampere Pulse Technology and Applications* (Sarov: VNIIEF, 1997)
64. Selemir V D, Plyashkevich L N (Eds) *Megagauss-9* (Sarov: VNIIEF, 2004)